

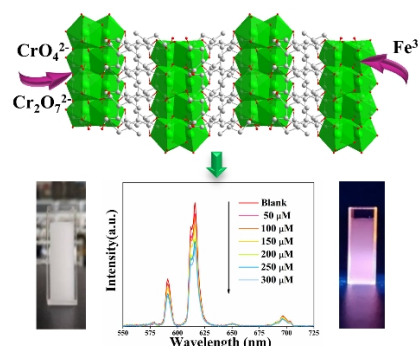
An Ultra-stable Eu^{3+} Doped Yttrium Coordination Polymer with Dual-function Sensing for Cr(VI) and Fe(III) Ions in Aqueous Solution

Fazheng Huang^{1†}, Xinhao Li^{1†}, Zhen Zhang^{1†}, Ziqi Jiang¹, Guoqiang Wang¹, Lingyun Li^{1*} and Yan Yu^{1*}

¹Key Laboratory of Advanced Materials Technology, College of Materials Science and Engineering, Fuzhou University, Fuzhou 350108, China

ABSTRACT The exploration of a dual-functional sensor is the key to effectively detect the Cr(VI) and Fe(III) cations in water, which is important to human health and environmental sustainability. Because of the phase stability and excellent luminescence, the rare-earth coordination polymers have great potential as dual-functional sensors. Here, we develop a $\text{Y}_{0.91}\text{Eu}_{0.09}(\text{H}_2\text{O})_2[\text{C}_6\text{H}_3(\text{CO}_2)_3](\text{MIL-92(Y):9\%Eu}^{3+})$ -based dual-function luminescent sensor on Cr(VI) and Fe(III) , which exhibits excellent phase stability and dispersibility in water. The luminescence of $\text{MIL-92(Y):9\%Eu}^{3+}$ aqueous suspension quenches on Fe^{3+} with Stern-Volmer constant K_{SV} of $1.79 \times 10^3 \text{ M}^{-1}$ and limit of detection of $17 \mu\text{M}$. The $\text{MIL-92(Y):9\%Eu}^{3+}$ aqueous suspension also has turn-off sensing ability towards $\text{Cr}_2\text{O}_7^{2-}$ and CrO_4^{2-} with K_{SV} values of 3.5×10^3 and $6.14 \times 10^3 \text{ M}^{-1}$, respectively. It has detection limitations of 10 and $5 \mu\text{M}$ on $\text{Cr}_2\text{O}_7^{2-}$ and CrO_4^{2-} ions, respectively.

Keywords: Cr(VI) , Fe(III) , luminescence sensing, dual-function detection, MIL-92



INTRODUCTION

The monitoring and elimination of Cr(VI) ($\text{Cr}_2\text{O}_7^{2-}$ and CrO_4^{2-}) in the drinking and ground water are an important content of environmental protection. Even at low concentrations, long term exposure to Cr(VI) ions can cause several health issues such as allergic reactions, hereditary genetic defects, and even lung cancer. Meanwhile, the detection and monitoring of Fe(III) (Fe^{3+}) in water are also crucial for human health, since the deficiency and overdose of Fe^{3+} cause hazards to human body. According to the U. S. national primary drinking water regulations (NPDWR), the maximum contaminant levels of chromium and iron in drinking water are 0.1 and 0.3 mg/L, respectively. The enforceable standard of Cr(VI) in drinking water and drinkable ground water is 0.05 mg/L, according to the Chinese quality standard for ground water (GB/T 14848-93) and quality standard for drinking water (GB5749-2006). Many technologies have been developed to detect Cr(VI) and Fe(III) ions in water system, such as flame atomic absorption spectrophotometric method,^[1,2] Raman spectrometer method^[3,4] and luminescence probe.^[5-8] Among them, the luminescence sensor based on the response of luminescence on the contaminant ion is a promising one because of their dual-function ability to detect both Cr(VI) and Fe(III) in water with high selectivity and sensitivity.

The luminescent metal coordination polymer-based dual-function sensors have attracted intensive research interest.^[9-15] Many luminescent metal coordination polymers are phase stability in water, which is the basis of contaminant detection in aqueous solutions. On the other hand, the luminescent metal ions in coordination polymer could be exchanged by cations such as Fe^{3+} or Cr^{3+} , leading to luminescence quenching and thus the sensing of these cations in water. Hence, the coordination polymer $\text{Y}_{1-x}\text{Eu}_x(\text{H}_2\text{O})_2[\text{C}_6\text{H}_3(\text{CO}_2)_3](\text{MIL-92(Y):}x\%\text{Eu}^{3+})$ is a potential candidate for dual-functional sensing.^[16] The ligand of trimellitic

acid with a simple and asymmetric spatial configuration give rise to the compact and dense structure of $\text{MIL-92(Y):}x\%\text{Eu}^{3+}$. The detection ability of a sensing material is usually determined by the Stern-Volmer constant K_{SV} and the limit of detection (LOD).^[17,18] The value of K_{SV} is calculated by $I_0/I = K_{\text{SV}}[Q] + 1$, where I_0 is the luminescence intensity of sensor before testing, I is the luminescence intensity of sensor with the appearance of targeted ion and $[Q]$ is the concentration of the targeted ion in aqueous solution. The value of K_{SV} reveals the intrinsic sensing ability of the rare-earth coordination polymer. The value of LOD is calculated via $\text{LOD} = 3\delta/K_{\text{SV}}$, where δ is the standard deviation of ten blank experiments for the luminescence intensity of the sensor. Thus, the value of LOD of a rare-earth coordination polymer-based luminescent sensor also depends on the dispersibility of the rare-earth coordination polymer in water, since the value of δ depends on the luminescence stability of aqueous suspension containing rare-earth coordination polymer. Recently, the luminescence sensing characteristics of Eu^{3+} doped coordination polymers $\text{Y}_{10}(\text{C}_8\text{H}_4\text{O}_4)_6(\text{CO}_3)_3(\text{OH})_{12}$ and $\text{Al}_{12}\text{O}(\text{OH})_{18}(\text{H}_2\text{O})_3(\text{Al}_2(\text{OH})_4)[\text{btc}]_6 \cdot 24\text{H}_2\text{O}$, which have different crystal structures from $\text{MIL-92(Y):}x\%\text{Eu}^{3+}$, have been studied by our research group.^[19,20] Both the luminescent coordination polymers are water stable and sensitive to Fe(III) or Cr(VI) ions. However, they show a limited sensitivity because of the low water dispersibility. Thus, improving the water dispersibility is crucial to obtaining a $\text{MIL-92(Y):}x\%\text{Eu}^{3+}$ -based dual-functional sensor.

In this work, the $\text{MIL-92(Y):9\%Eu}^{3+}$ -based dual-function sensor for Cr(VI) and Fe(III) was obtained for the first time. The $\text{MIL-92(Y):9\%Eu}^{3+}$ powders have phase and luminescence stability in aqueous solution with pH values ranging from 4 to 11. The powders are stable even soaked in water for 5 days. Because of using polyvinylpyrrolidone (PVP) as a surfactant, the $\text{MIL-92(Y):9\%Eu}^{3+}$ powders show good water dispersibility. The luminescence of aqueous suspension containing $\text{MIL-92(Y):9\%Eu}^{3+}$ powder remains

nearly unchanged in 20 minutes. The suspension displays luminescence quenching towards Fe^{3+} , $\text{Cr}_2\text{O}_7^{2-}$ and CrO_4^{2-} ions with K_{SV} values of 1.79×10^3 , 3.5×10^3 and $6.14 \times 10^3 \text{ M}^{-1}$, respectively. As a result, the MIL-92(Y):9% Eu^{3+} -based luminescence sensor shows detection limitations of 17, 10 and 5 μM towards Fe^{3+} , $\text{Cr}_2\text{O}_7^{2-}$ and CrO_4^{2-} ions, respectively.

n RESULTS AND DISCUSSION

Morphology, Phase and Optical Spectroscopic Properties of Eu^{3+} Doped MIL-92(Y). Figure 1a displays the crystal structure of the low-temperature phase MIL-92(Y), which has a compact structure and crystallizes in the $C2/c$ space group with cell parameters of $a = 16.428(1)$, $b = 6.071(1)$, $c = 20.404(1) \text{ \AA}$, $\beta = 95.31(3)^\circ$.^[16] The compact structure of MIL-92(Y) crystal is composed by inorganic $\{\text{YO}_8\}$ layers connected by deprotonated trimellitic acid ligands. As seen from Figure S1, the inorganic $\{\text{YO}_8\}$ layer consists of upper and lower staggered $\{\text{YO}_8\}$ polyhedra, which are bridged by the carboxyl groups. Meanwhile, there is only one kind of Y^{3+} ion, which is coordinated by eight oxygen atoms with bond lengths ranging from 2.292 to 2.817 \AA . Eu^{3+} doped MIL-92(Y) samples can be obtained by using $\text{Eu}(\text{NO}_3)_3 \cdot 6\text{H}_2\text{O}$ as the starting material to replace partial $\text{Y}(\text{NO}_3)_3 \cdot 6\text{H}_2\text{O}$. The introduction of Eu^{3+} makes MIL-92(Y) samples brightly luminescent (Figure 1b). As shown in Figure 1c, the PXRD patterns of MIL-92(Y):x% Eu^{3+} samples match well with the simulated pattern of MIL-92(Y), indicating the successful doping of Eu^{3+} ions. The TEM images of MIL-92(Y):9% Eu^{3+} particles are displayed in Figure 1d, which clearly demonstrates the coating of PVP. The existence of PVP on the particle surface could be verified by the XPS and FT-IR data, as shown in Figure S2 and S3. The nitrogen peak in the overall spectrum and the C–N binding band in the high resolution spectrum of C 1s reveal the existence of PVP (Figure S2). The optical absorption can confirm this at 1290 and 1677 cm^{-1} in the FT-IR spectrum (Figure S3). The EDS scanning mapping shown in Figure 1e reveals the distribution of yttrium, oxygen, carbon, europium and nitrogen elements in and on the MIL-92(Y):9% Eu^{3+} particle. The above results confirm the successful preparation of PVP modified Eu^{3+} doped MIL-92(Y) samples. What's more, the compact structure and inorganic $\{\text{YO}_8\}$ layers make MIL-92(Y) crystal an ideal host to be doped with Eu^{3+} for the high efficient luminescence.

The typical photo-luminescence spectra of Eu^{3+} doped MIL-

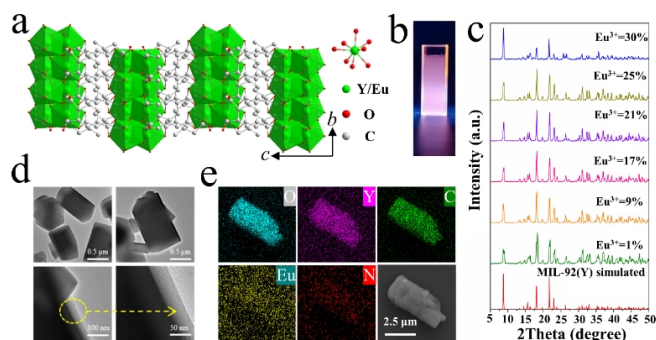


Figure 1. Crystal structure (a), luminescent images (b), PXRD patterns (c), TEM images (d) and EDS scanning mapping (e) of MIL-92(Y) and Eu^{3+} doped samples

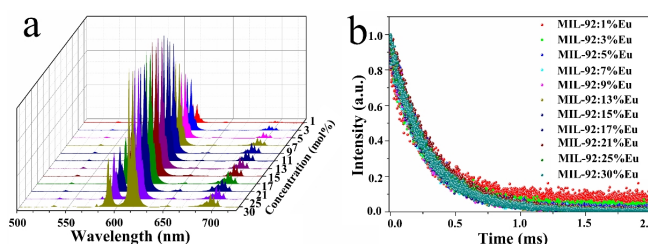


Figure 2. The Eu^{3+} concentration dependent luminescence spectra (a) and decay curves (b) of MIL-92(Y):x% Eu^{3+} samples.

92(Y) are shown in Figure S4a. The excitation and emission spectra of Eu^{3+} doped MIL-92(Y) consist of a band (280–350 nm) assigned to the ligand absorption and peaks (350–500 nm) belonging to the transitions of Eu^{3+} , which is summarized in Figure S4b.^[21–23] When excited, the Eu^{3+} ions will be pumped from the ground state $^7\text{F}_0$ to the upper levels such as $^5\text{D}_4$, $^5\text{L}_7$, $^5\text{L}_6$, $^5\text{D}_3$ and $^5\text{D}_2$. With the assistance of non-radiative transitions mainly caused by the lattice vibrating, the excited Eu^{3+} will relax to the metastable levels such as $^5\text{D}_1$ and $^5\text{D}_0$. The optical emission occurs when Eu^{3+} radiatively relaxes from the metastable manifolds to the lowered states of $^7\text{F}_j$ ($j = 0, 1, 2, 3, 4$). Figure 2a and 2b show the Eu^{3+} concentration dependent optical emission spectra and luminescence decay curves. The optical emission increases first and reaches the maximum when the content of Eu^{3+} is 9% (mol ratio). It decreases when the content of Eu^{3+} exceeds 20%. On the other hand, the luminescence decay curves of MIL-92(Y):x% Eu^{3+} samples display a first-order exponential decay manner, with a lifetime of the $^5\text{D}_0$ state of $280 \pm 20 \text{ ns}$. Based on the above results, the MIL-92(Y):9% Eu^{3+} sample was used in the further investigation in this work.

Phase Stability and Dispersibility of MIL-92(Y):9% Eu^{3+} in Water. Benefitting from the modified surface, the MIL-92(Y):9% Eu^{3+} powders with Zeta potential of 12.8 mV have good dispersibility in water, as shown in Figure 3a–d. The luminescence intensity of MIL-92(Y):9% Eu^{3+} suspension rarely changes within 20 min after

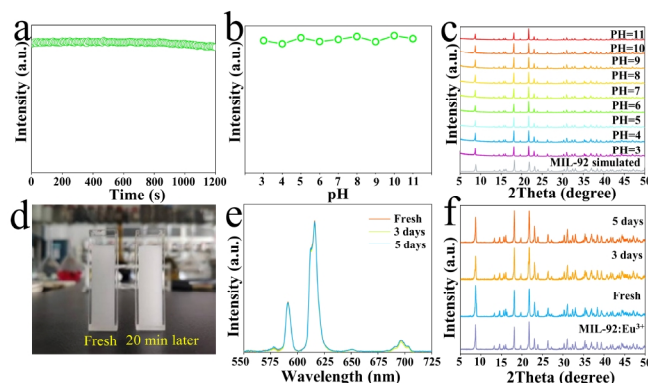


Figure 3. The time dependent (a) and pH dependent (b) luminescence intensity of MIL-92(Y):9% Eu^{3+} aqueous suspension. PXRD patterns of MIL-92(Y):9% Eu^{3+} powders immersed in water with different pH values (c). Photo of the MIL-92(Y):9% Eu^{3+} aqueous suspension (d). The luminescence spectra of the suspension 3 and 5 days after the formation of suspension (e) and PXRD patterns of the immersed MIL-92(Y):9% Eu^{3+} particles (f).

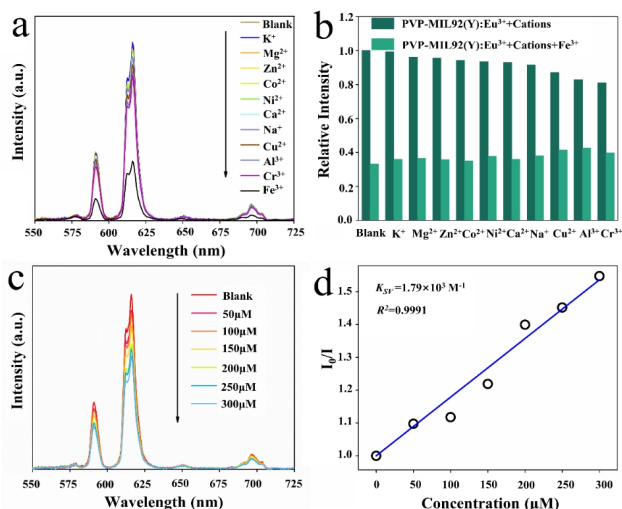


Figure 4. Luminescence spectra of MIL-92(Y):9%Eu³⁺ suspension with metal ions (a) and anti-interference luminescence quenching of MIL-92(Y):9%Eu³⁺ suspension (b). Luminescence spectra of MIL-92(Y):9%Eu³⁺ suspension containing Fe³⁺ ion with different concentrations (c) and the corresponding Stern-Volmer plot fitting result (d).

the formation of the suspension. The MIL-92(Y):9%Eu³⁺ suspension also has excellent pH stability. Figure 3b shows the pH dependent luminescence intensity of MIL-92(Y):9%Eu³⁺ suspension, which keeps nearly unchanged with pH values ranging from 3 to 11. Meanwhile, the phase of MIL-92(Y):9%Eu³⁺ powder keeps stable after being immersed in the aqueous solutions (Figure 3c). Figure 3e and 3f display the long-term luminescence stability of the MIL-92(Y):9%Eu³⁺ suspension, which exhibits excellent stability even 5 days after the formation of the aqueous solution. The dispersibility of MIL-92(Y):9%Eu³⁺ in water comes from the surfactant PVP molecule, the existence of which is confirmed by TEM, FT-IR and XPS measurements. The MIL-92(Y):9%Eu³⁺ powder could also be prepared without using PVP as a surfactant. However, the MIL-92(Y):9%Eu³⁺ powders prepared without PVP show poor dispersibility in water. As shown in Figure S5, the suspension is unstable with luminescence completely quenched in 5 min, since the Zeta potential is only 0.2 mV. The phase stability and water dispersibility are the basis of MIL-92(Y):9%Eu³⁺ powders for analyte detection in water.^[24-26]

Dual-functional Sensing Ability of MIL-92(Y):9%Eu³⁺ in Aqueous Solution.

The MIL-92(Y):9%Eu³⁺ powder has sensing ability on Fe³⁺ ions. The MIL-92(Y):9%Eu³⁺ aqueous suspension containing Fe³⁺ (2 mM) displays obvious luminescence quenching, as shown in Figure 4a. Meanwhile, the luminescence of MIL-92(Y):9%Eu³⁺ aqueous suspension rarely changes at the presence of other cations such as K⁺, Na⁺, Zn²⁺, Mg²⁺, Ca²⁺, Co²⁺, Ni²⁺, Cu²⁺, Al³⁺ and Cr³⁺. Moreover, the luminescence quenching of MIL-92(Y):9%Eu³⁺ on Fe³⁺ is not affected by the other cations, showing good anti-interference sensing capability (Figure 4b). As seen from Figure 4c, the luminescence intensity of MIL-92(Y):9%Eu³⁺ aqueous suspension containing Fe³⁺ ion decreases gradually with the increase of Fe³⁺ concentration. In the Fe³⁺ ion concentration range of 0–300 nM, the luminescence intensity at

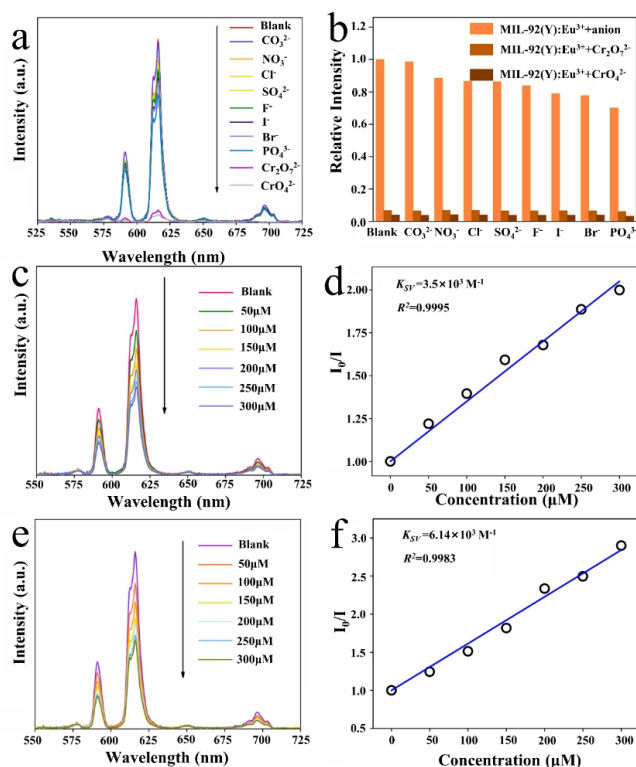


Figure 5. Luminescence spectra of MIL-92(Y):9%Eu³⁺ suspension with different anions (a) and anti-interference luminescence quenching of MIL-92(Y):9%Eu³⁺ suspension (b). Luminescence spectra of MIL-92(Y):9%Eu³⁺ suspension contained Cr₂O₇²⁻ with different concentrations (c) and the corresponding Stern-Volmer plot fitting result (d). Luminescence spectra of MIL-92(Y):9%Eu³⁺ suspension contained CrO₄²⁻ with different concentrations (e) and the corresponding Stern-Volmer plot fitting result (f).

616 nm could be fitted well by the Stern-Volmer equation with $K_{SV} = 1.79 \times 10^3 \text{ M}^{-1}$ and $R^2 = 0.9991$ (Figure 4d). Thus, the MIL-92(Y):9%Eu³⁺ has a LOD value of 17 μM towards the Fe³⁺ ion.

The MIL-92(Y):9%Eu³⁺ powder shows detection ability on Cr₂O₇²⁻ and CrO₄²⁻ ions. When dispersed into aqueous solutions containing anions such as F⁻, Cl⁻, Br⁻, I⁻, SO₄²⁻, CO₃²⁻, NO₃⁻, PO₄³⁻, CrO₄²⁻ and Cr₂O₇²⁻ with the concentration of 2 mM, only the MIL-92(Y):9%Eu³⁺ suspensions with Cr₂O₇²⁻ and CrO₄²⁻ ions quench, as shown in Figure 5a. The luminescence quenching of MIL-92(Y):9%Eu³⁺ suspensions on Cr₂O₇²⁻ and CrO₄²⁻ is not influenced by the other anions (Figure 5b). Although the luminescence of MIL-92(Y):9%Eu³⁺ suspension quenches at the presence of Cr₂O₇²⁻ and CrO₄²⁻, it shows different sensitivity on them. As shown in Figure 5c and 5d, the MIL-92(Y):9%Eu³⁺ suspension has a quantitative detection capability on Cr₂O₇²⁻ with K_{SV} and LOD values of $3.5 \times 10^3 \text{ M}^{-1}$ and 10 μM, respectively. For the case of CrO₄²⁻ shown in Figure 5e and 5f, the MIL-92(Y):9%Eu³⁺ suspension exhibits a higher quantitative detection capability with K_{SV} and LOD values of $6.14 \times 10^3 \text{ M}^{-1}$ and 5 μM, respectively. The R^2 values of 0.9995 and 0.9983 shown in Figure 5d and 5f demonstrate good linear fitting between the luminescence quenching of MIL-92(Y):9%Eu³⁺ suspension and the targeted ion concentrations.

Table 1. K_{SV} , LOD and Quenching Efficiency of Serial Coordination Polymer-based Dual-functional Luminescence Sensors on Fe^{3+} and $Cr(IV)$

Compound name	K_{SV} (M^{-1})			LOD (μM)			Quenching efficiency (%, at 1 mM)			Ref.
	Fe^{3+}	CrO_4^{2-}	$Cr_2O_7^{2-}$	Fe^{3+}	CrO_4^{2-}	$Cr_2O_7^{2-}$	Fe^{3+}	CrO_4^{2-}	$Cr_2O_7^{2-}$	
[Cd(4-bmnpd(2-NBA) ₂)]	30430	44470	31800	99	69	100	96.8%	97.8%	96.9%	27
{[Zn(L)(bpp)]·DMF} _n	25600	—	2780	0.76	—	3.52	96.2%	—	73.5%	28
{[Cd ₂ (L) ₂ (bpe) ₂]·3DMF·2.5H ₂ O} _n	17400	—	3700	0.61	—	1.65	94.6%	—	78.7%	29
{[Zn(L)(H ₂ O) ₂]·H ₂ O} _n	109000	41000	91000	0.56	5.7	7.3	99.1%	97.6%	98.9%	30
{[Cd ₂ (bptc)(4,4'-bipy)-(H ₂ O) ₂]·4H ₂ O} _n	6210	5340	9340	20.3	16	13.6	86.1%	84.2%	90.3%	31
[Cd _{1.5} (L) ₂ (bpy)(NO ₃)]·2DMF·2H ₂ O	11300	17300	54200	0.13	0.95	1.09	91.9%	94.5%	98.2%	32
{[Zn(L)(bimb)]·2H ₂ O} _n	166000	49400	—	0.18	0.61	—	99.4%	98.0%	—	33
MIL-92(Al):Eu ³⁺	79400	—	7290	0.793	—	41	98.8%	—	87.9%	34
MIL-92(Y):Eu ³⁺	1790	6140	3500	17	5	10	64.2%	86.0%	77.8%	This work

On the other hand, about half of the MIL-92(Y):9%Eu³⁺ powders were lost after a sensing test on CrO_4^{2-} , $Cr_2O_7^{2-}$ or Fe^{3+} . The main reason for this consumption is the unavoidable loss during the vacuum suction filtration process to separate MIL-92(Y):9%Eu³⁺ powders from the tested solution.

The detection efficiency (or quenching efficiency) on analyte with concentration of $[Q]$ could be obtained according to $(1-I/I_0) \times 100\%$. The parameters such as K_{SV} , LOD and quenching efficiency of serial coordination polymer-based dual-functional sensors are listed in Table 1. The detection limits of MIL-92(Y):9%Eu³⁺-based sensor towards Fe^{3+} , CrO_4^{2-} and $Cr_2O_7^{2-}$ ions are in the middle level among the listed dual-functional sensors. The [Cd_{1.5}(L)₂(bpy)(NO₃)]·2DMF·2H₂O-based sensor has the best sensing ability towards Fe^{3+} , CrO_4^{2-} and $Cr_2O_7^{2-}$ with LOD of 0.13, 0.95 and 1.09 μM . On the other hand, the MIL-92(Y):9%Eu³⁺-based sensor has smaller values of K_{SV} on Fe^{3+} , CrO_4^{2-} and $Cr_2O_7^{2-}$ ions, leading to smaller luminescence quenching efficiencies of 64.2%, 86.0% and 77.8% towards Fe^{3+} , CrO_4^{2-} and $Cr_2O_7^{2-}$ ions with the concentration of 1 mM. The larger detection limit is the disadvantage of MIL-92(Y):9%Eu³⁺ as a dual-functional sensor. As discussed above, the value of LOD is deter-

mined via $3\delta/K_{SV}$, where K_{SV} is a kind of internal indicator dependent on the quenching mechanism. Hence, reducing the value of the standard deviation of ten blank experiments for the luminescence intensity of the sensor (δ) is an effective way to improve the detection limit of MIL-92(Y):9%Eu³⁺-based sensor. From the viewpoint of materials science, controlling the MIL-92(Y):9%Eu³⁺ particle size to be nanometer level and further improving its dispersibility in water are the effective approaches to reduce the value of δ and improve the sensing ability. On the other hand, the relative less luminescence quenching of MIL-92(Y):9%Eu³⁺ on Fe^{3+} , CrO_4^{2-} and $Cr_2O_7^{2-}$ ions indicates that it could work in a larger concentration range when detecting these analytes, which is a major advantage of MIL-92(Y):9%Eu³⁺-based luminescence sensor.^[27-34]

Possible Mechanism of Luminescence Quenching. Considering the strong absorption of CrO_4^{2-} and $Cr_2O_7^{2-}$ ions on the light with the wavelength from 200 to 400 nm (Figure S6), the inner filter effect is the possible reason for the luminescence quenching of MIL-92(Y):9%Eu³⁺ suspension at the presence of CrO_4^{2-} and $Cr_2O_7^{2-}$ ions. The optical absorptions of aqueous solutions containing anions such as F^- , Cl^- , Br^- , I^- , SO_4^{2-} , CO_3^{2-} , NO_3^- , PO_4^{3-} , CrO_4^{2-} and $Cr_2O_7^{2-}$ are displayed in Figure S6, as well as the excitation and emission spectra of MIL-92(Y):9%Eu³⁺. Only the CrO_4^{2-} and $Cr_2O_7^{2-}$ ions have strong absorption during 200–400 nm, overlapping with the excitation spectrum of MIL-92(Y):9%Eu³⁺. In other words, the competitive optical absorption of CrO_4^{2-} or $Cr_2O_7^{2-}$ ions hinders the excitation of Eu³⁺, which is the reason for the luminescence quenching. Figure 6a and 6b show the luminescence branching ratios of MIL-92(Y):9%Eu³⁺ powder after being immersed in the aqueous solution containing CrO_4^{2-} and $Cr_2O_7^{2-}$ ions. The luminescence intensity ratios of transitions from 5D_0 to 7F_1 , 7F_2 and 7F_4 levels rarely change via the increase of CrO_4^{2-} and $Cr_2O_7^{2-}$ concentration. This result demonstrates that the local circumstance of Eu³⁺ keeps unchanged during the sensing of CrO_4^{2-} and $Cr_2O_7^{2-}$, confirming the inner filter effect caused luminescence quenching. During the sensing experiment on CrO_4^{2-} and $Cr_2O_7^{2-}$, the luminescence of MIL-92(Y):9%Eu³⁺-based sensor can rapidly recover for at least 5 cycles with water washing, as depicted in Figure 6c and 6d. The luminescence recovery of MIL-92(Y):9%Eu³⁺-based sensor indicates no chemical reaction between MIL-92(Y):9%Eu³⁺ and CrO_4^{2-} , $Cr_2O_7^{2-}$. The recovery of the luminescence and unchanged luminescence

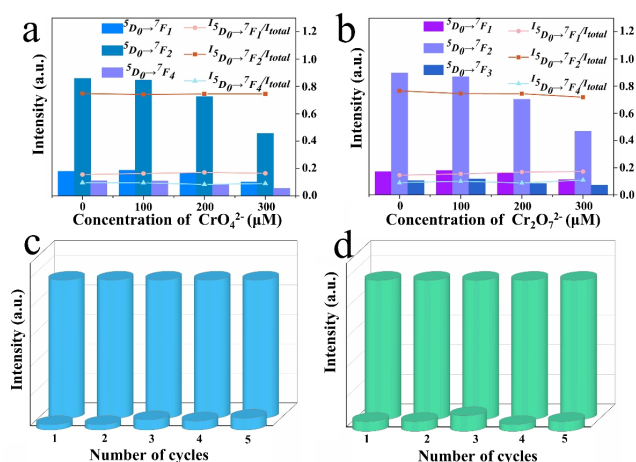


Figure 6. Luminescence branch ratios of MIL-92(Y):9%Eu³⁺ suspension containing different contents of CrO_4^{2-} ion (a) and $Cr_2O_7^{2-}$ ion (b). Five cycle tests of luminescent MIL-92(Y):9%Eu³⁺ sensing on CrO_4^{2-} (c) and $Cr_2O_7^{2-}$ (d) ions.

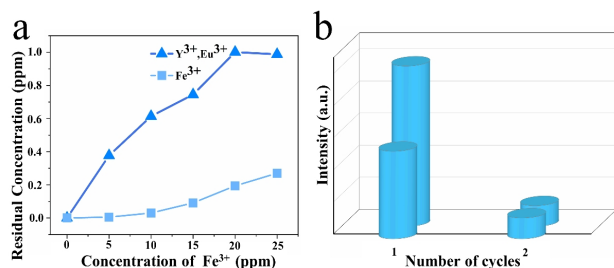


Figure 7. Residual concentrations of Re^{3+} ($\text{Re}^{3+} = \text{Y}^{3+} + \text{Eu}^{3+}$) and Fe^{3+} in the filtrate solution after the luminescence quenching test (a) and cycle tests of luminescent MIL-92(Y):9% Eu^{3+} sensing on Fe^{3+} ions (b).

branching ratios after sensing CrO_4^{2-} and $\text{Cr}_2\text{O}_7^{2-}$ ions demonstrate that the inner filter effect is the reason for luminescence quenching of MIL-92(Y):9% Eu^{3+} -based sensor.^[31-34]

The dynamic changes of cation concentration in the MIL-92(Y):9% Eu^{3+} suspensions containing Fe^{3+} are displayed in Figure 7a. After the separation of MIL-92(Y):9% Eu^{3+} powders, there are no Fe^{3+} ions or trace amount of Fe^{3+} left in the filtrate. However, the rare earth ions $\text{Y}^{3+}/\text{Eu}^{3+}$ come out from the MIL-92(Y):9% Eu^{3+} particles. The concentration of rare earth ion left in the filtrate enhances as the starting concentration of Fe^{3+} increases. This validates that ion exchange between Fe^{3+} and $\text{Y}^{3+}/\text{Eu}^{3+}$ happens during the sensing experiment on Fe^{3+} . Meanwhile, the luminescence of MIL-92(Y):9% Eu^{3+} cannot recover after the sensing test on Fe^{3+} ion. As shown in Figure 7b, the intense emission of MIL-92(Y):9% Eu^{3+} -based sensor cannot be repeated once it contacts with Fe^{3+} ion in aqueous solution. These results demonstrate that the ion-exchange between $\text{Eu}^{3+}/\text{Y}^{3+}$ and Fe^{3+} is the possible reason for the luminescence quenching of MIL-92(Y):9% Eu^{3+} -based sensor on Fe^{3+} .^[35-39]

CONCLUSION

A dual-function luminescent sensor has been explored based on the PVP modified MIL-92(Y):9% Eu^{3+} crystal. The phase stability and water dispersibility make MIL-92(Y):9% Eu^{3+} suspension an ideal sensor for Fe^{3+} , $\text{Cr}_2\text{O}_7^{2-}$ and CrO_4^{2-} . The luminescence of MIL-92(Y):9% Eu^{3+} aqueous suspension quenches on Fe^{3+} with K_{sv} value of $1.79 \times 10^3 \text{ M}^{-1}$ and detection limitation of $17 \mu\text{M}$. The ion exchange between $\text{Y}^{3+}/\text{Eu}^{3+}$ and Fe^{3+} is the possible reason for the luminescence quenching of MIL-92(Y):9% Eu^{3+} on Fe^{3+} . The luminescence of MIL-92(Y):9% Eu^{3+} aqueous suspension also quenches at the presence of $\text{Cr}_2\text{O}_7^{2-}$ and CrO_4^{2-} . The K_{sv} values of MIL-92(Y):9% Eu^{3+} aqueous suspension on $\text{Cr}_2\text{O}_7^{2-}$ and CrO_4^{2-} ions are 3.5×10^3 and $6.14 \times 10^3 \text{ M}^{-1}$, leading to the detection limitations of 10 and $5 \mu\text{M}$, respectively. The inner filter effect is the possible reason for the luminescence quenching on $\text{Cr}_2\text{O}_7^{2-}$ and CrO_4^{2-} ions. The dual-functional detection ability of MIL-92(Y):9% Eu^{3+} on Fe(III) and Cr(VI) demonstrates that: (1) Using PVP as surfactant can improve the dispersibility of MIL-92 type metal coordination polymer; (2) The phase stability and water dispersibility are the keys to exploring a sensing material to detect contaminations in water with high K_{sv} value and lower limit of detection.

EXPERIMENTAL

Materials. Yttrium nitrate hexahydrate ($\text{Y}(\text{NO}_3)_3 \cdot 6\text{H}_2\text{O}$, 99.5%), europium nitrate hexahydrate ($\text{Eu}(\text{NO}_3)_3 \cdot 6\text{H}_2\text{O}$, 99.5%), 1,2,4-benzenetricarboxylic acid (trimellitic acid, 98%), sodium acetate (NaAc, 99%) and polyvinylpyrrolidone (PVP, 98%) were purchased from Aladdin Reagent Co., Ltd. and used as received without further purification. Deionized water was used throughout the experiments.

Preparation of Eu^{3+} Doped MIL-92(Y). The MIL-92(Y):x% Eu^{3+} samples were prepared through the hydrothermal method.^[16] Rare-earth nitrates, trimellitic acid, sodium acetate and PVP were used as starting materials with the ratio of rare-earth nitrates:trimellitic acid:sodium hydroxide:water to be 1:1:2:180 (mol). To control the particle size and improve the water dispersibility, PVP was used as the surfactant. Firstly, the $\text{Y}(\text{NO}_3)_3 \cdot 6\text{H}_2\text{O}$, $\text{Eu}(\text{NO}_3)_3 \cdot 6\text{H}_2\text{O}$, NaAc and trimellitic acid powders were added into 6.48 mL of H_2O and stirred for 20 min. During this procedure, 240 μL PVP aqueous solution (10 mM) was added into the mixture. Then, the mixture was moved into a Teflon-lined autoclave to perform a hydrothermal reaction at 220°C for 2 h. After cooling to room temperature, the precipitate was collected by centrifugation at 8000 rpm and washed with deionized water. Finally, the MIL-92(Y):x% Eu^{3+} powders were obtained after drying in a vacuum oven at 60°C for 2 h. The MIL-92(Y):x% Eu^{3+} powders could be prepared via the above procedure with pH value of the solvent ranging from 3 to 9.

Characterization. Powder X-ray diffraction (PXRD) patterns of the MIL-92(Y):x% Eu^{3+} powders were collected by using a Mini-Flex 600 X-ray diffractometer (Rigaku Corporation, Japan) with $\text{CuK}\alpha$ radiation ($\lambda = 0.154 \text{ nm}$) at 40 kV and 15 mA. The scan range of 2 theta was 5° – 70° . The energy-dispersive X-ray spectrum (EDS) was measured on a field emission scanning electron microscope (SEM SUPRA 55, Carl Zeiss, German). The images of the nanoparticles were taken on a Talos F200i type transmission electron microscope (TEM). Fourier transform infrared spectrum (FT-IR, KBr pellets) of compound MIL-92 was recorded using a Nicolet 5700 FT-IR spectrometer. Zeta potential (ξ) was determined by dynamic light scattering analysis (Zetasizer Nano ZS-90). Optical excitation and emission spectra were recorded on a Fluoro-Max-4 fluorescence spectrophotometer (HORIBA Jobin Yvon Co.). The X-ray Photoelectron Spectroscopy (XPS) spectra were recorded on a Thermo Scientific K-Alpha type Spectrometer.

Luminescence Stability and Sensing Experiment. To monitor the luminescence stability of the aqueous suspension containing MIL-92(Y):9% Eu^{3+} powders, the luminescence spectra were recorded with an interval time of 10 second. The pH dependent luminescence of the suspension was recorded using suspensions with different pH values. The aqueous suspensions with different pH values were shaken well before recording the luminescence spectrum. Meanwhile, the long-term luminescence stability of the suspension was also studied by recording the optical emission of MIL-92(Y): 9% Eu^{3+} powders after they were soaked in water for 3 and 5 days. Luminescence quenching experiment was conducted to investigate the detection ability of MIL-92(Y):9% Eu^{3+} . A 5 mL amount of 2 mM MCl n ($M^{n+} = \text{Na}^+, \text{K}^+, \text{Mg}^{2+}, \text{Cu}^{2+}, \text{Ca}^{2+}, \text{Zn}^{2+}, \text{Ni}^{2+}$,

Co^{2+} , Al^{3+} , Cr^{3+} , Fe^{3+} , $n = 1, 2, 3$) solution was loaded into a centrifuge tube for sensing experiments. Several servings of 5 mg MIL-92(Y):9% Eu^{3+} powders were dispersed into the different cation solutions listed above. After the addition of MIL-92(Y):9% Eu^{3+} powders, the luminescence spectrum of the suspension was recorded in 5 min. To investigate the influence of other cations for the selectively quenching response, MIL-92(Y):9% Eu^{3+} powders were also dispersed in the mixture solution containing the above cations with and without Fe^{3+} ions. The concentration of both the interfering ion and Fe^{3+} is 2 mM in the interfering test. The luminescence sensing of MIL-92(Y): 9% Eu^{3+} on the $\text{Cr}_2\text{O}_7^{2-}$ and CrO_4^{2-} anions was performed in a similar way.

The luminescence recoverability of MIL-92(Y):9% Eu^{3+} after the sensing on Fe^{3+} , $\text{Cr}_2\text{O}_7^{2-}$ and CrO_4^{2-} was also tested. During the CrO_4^{2-} and $\text{Cr}_2\text{O}_7^{2-}$ test, a serving of 20 mg MIL-92(Y):9% Eu^{3+} powders was added into 3 mL water to form a stable luminescence suspension, the emission intensity of which was recorded as the initial intensity of cycle 1. At the beginning of the quenching and recovery cycle test, MIL-92(Y):9% Eu^{3+} powders were separated from the suspension via vacuum filtration and then added into 3 mL aqueous solutions of CrO_4^{2-} or $\text{Cr}_2\text{O}_7^{2-}$ with concentration of 2 mM to form suspensions. The luminescence is quenched at the presence of CrO_4^{2-} or $\text{Cr}_2\text{O}_7^{2-}$ and the integrated emission intensity was recorded as quenched luminescence intensity of cycle 1. Then, the MIL-92(Y):9% Eu^{3+} powders were separated again from the suspensions containing CrO_4^{2-} or $\text{Cr}_2\text{O}_7^{2-}$ and washed by deionized water to perform the following luminescence recovery and quenching test. The cycle tests of luminescent MIL-92(Y):9% Eu^{3+} sensing on Fe^{3+} were performed similarly. A serving of 3 mg MIL-92(Y):9% Eu^{3+} powders was added into 3 mL water to form a stable luminescence suspension, the emission intensity of which was recorded as the initial intensity of cycle 1. The MIL-92(Y):9% Eu^{3+} powders were separated from the suspension via vacuum filtration and then added into 3 mL aqueous solutions of Fe^{3+} with the concentration of 2 mM to form a suspension. The luminescence is quenched at the presence of Fe^{3+} and the integrated emission intensity was recorded as quenched luminescence intensity of the first cycle. Then, the MIL-92(Y):9% Eu^{3+} powders were separated from the suspensions containing Fe^{3+} and washed with deionized water to perform the following luminescence recovery and quenching test.

ACKNOWLEDGEMENTS

This research was supported by the National Natural Science Foundation of China (51972061).

AUTHOR CONTRIBUTION

[†] These authors contributed equally to this work

AUTHOR INFORMATION

Corresponding authors. Emails: lilingyun@fzu.edu.cn and yuyan@fzu.edu.cn

COMPETING INTERESTS

The authors declare no competing interests.

ADDITIONAL INFORMATION

Supplementary information is available for this paper at <http://manu30.magtech.com.cn/jghx/EN/10.14102/j.cnki.0254-5861.2021-0071>

For submission: <https://mc03.manuscriptcentral.com/cjsc>

REFERENCES

- (1) Yebra, M. C.; Cespon, R. M.; Moreno-Cid, A. Automatic determination of ascorbic acid by flame atomic absorption spectrometry. *Anal. Chim. Acta* **2001**, 448, 157–164.
- (2) Monteiro, M. I. C.; Fraga, I. C. S.; Yallouz, A. V.; de Oliveira, N. M. M.; Ribeiro, S. H. Determination of total chromium traces in tannery effluents by electrothermal atomic absorption spectrometry, flame atomic absorption spectrometry and UV-visible spectrophotometric methods. *Talanta* **2002**, 58, 629–633.
- (3) Li, Z.; Deen, M. J.; Kumar, S.; Selvaganapathy, P. R. Raman spectroscopy for in-line water quality monitoring-instrumentation and potential. *Sensors* **2014**, 14, 17275–17303.
- (4) Song, C.; Yang, B.; Zhu, Y.; Yang, Y.; Wang, L. Ultrasensitive silver nanorods array SERS sensor for mercury ions. *Biosens. Bioelectron.* **2017**, 87, 59–65.
- (5) Ding, B.; Guo, C.; Liu, S. X.; Cheng, Y.; Wu, X. X.; Su, X. M.; Liu, Y. Y.; Li, Y. A unique multi-functional cationic luminescent metal-organic nanotube for highly sensitive detection of dichromate and selective high capacity adsorption of Congo red. *RSC Adv.* **2016**, 6, 33888–33900.
- (6) Karimi, M.; Badiei, A.; Mohammadi Ziarani, G. SBA-15 functionalized with naphthalene derivative for selective optical sensing of $\text{Cr}_2\text{O}_7^{2-}$ in water. *Anal. Sci.* **2016**, 32, 511–516.
- (7) Liu, J.; Ji, G.; Xiao, J.; Liu, Z. Ultraprecise 1D europium complex for simultaneous and quantitative sensing of Cr(III) and Cr(VI) ions in aqueous solution with high selectivity and sensitivity. *Inorg. Chem.* **2017**, 56, 4197–4205.
- (8) Liu, W.; Wang, Y.; Bai, Z.; Li, Y.; Wang, Y.; Chen, L.; Xu, L.; Diwu, J.; Chai, Z.; Wang, S. Hydrolytically stable luminescent cationic metal organic framework for highly sensitive and selective sensing of chromate anions in natural water systems. *ACS Appl. Mater. Interfaces* **2017**, 9, 16448–16457.
- (9) Yang, X. F.; Yu, D. Y.; Li, X. M.; Zhang, K. W.; Huang, W. H. Two 2D-MOFs based on two flexible ligands: structural control and fluorescence sensing on Fe^{III} cation and Cr^{VI} -containing anions. *J. Solid State Chem.* **2019**, 272, 166–172.
- (10) Pang, J. J.; Du, R. H.; Lian, X.; Yao, Z. Q.; Xu, J.; Bu, X. H. Selective sensing of Cr^{VI} and Fe^{III} ions in aqueous solution by an exceptionally stable Tb^{III}-organic framework with an AIE-active ligand. *Chin. Chem. Lett.* **2021**, 32, 2443–2447.
- (11) Yin, J. C.; Li, N.; Qian, B. B.; Yu, M. H.; Chang, Z.; Bu, X. H. Highly stable Zn-MOF with Lewis basic nitrogen sites for selective sensing of Fe^{3+} and $\text{Cr}_2\text{O}_7^{2-}$ ions in aqueous systems. *J. Coord. Chem.* **2020**, 73, 2718–2727.
- (12) Xu, C.; Bi, C.; Zhu, Z.; Luo, R.; Zhang, X.; Zhang, D.; Fan, C.; Cui, L.; Fan, Y. Metal-organic frameworks with 5,5'-(1,4-xylylenediamino) diisophthalic acid and various nitrogen-containing ligands for selectively sensing Fe^{III} /Cr(VI) and nitroaromatic compounds. *CrystEngComm* **2019**, 21, 2333–2344.
- (13) Qian, L. L.; Wang, Z. X.; Ding, J. G.; Tian, H. X.; Li, K.; Li, B. L.; Li, H. Y. A 2D copper(I) metal-organic framework: synthesis, structure and luminescence sensing for cupric, ferric, chromate and TNP. *Dyes Pigm.* **2020**, 175, 108159–108168.

- (14) Yang, G. P.; Luo, X. X.; Liu, Y. F.; Li, K.; Wu, X. L. [Co₃(μ₃-O)]-based metal-organic frameworks as advanced anode materials in K- and Na-ion batteries. *ACS Appl. Mater. Interfaces* **2021**, 13, 46902–46908.
- (15) Zhang, Y.; Qin, H. N.; Li, B. L.; Wu, B. Syntheses, structures and photocatalytic degradation properties of two copper(II) coordination polymers with flexible bis(imidazole) ligand. *Chin. J. Struct. Chem.* **2021**, 40, 595–602.
- (16) Surblé, S.; Serre, C.; Millange, F.; Pelle, F.; Férey, G. Synthesis, characterisation and properties of a new three-dimensional yttrium-europium coordination polymer. *Solid State Sci.* **2005**, 7, 1074–1082.
- (17) Li, L.; Chen, F. F.; Pan, J.; Zhong, S.; Li, L.; Yu, Y. Amino-functionalized YF₃:Eu³⁺ nanoparticles: a selective two-in-one fluorescent probe for Cr(III) and Cr(VI) detection. *J. Lumines.* **2020**, 226, 117440–117449.
- (18) Pan, J.; Zhong, K.; Zhang, Z.; Chen, W.; Lin, Y.; Wang, G.; Li, L.; Yu, Y. Using CaF₂:Eu³⁺ powder as a luminescent probe to detect Cr₂O₇²⁻ ions: a new application on the environmental conservation of an old optical material. *Opt. Mater. Express* **2018**, 8, 2782–2794.
- (19) Chen, W.; Li, L.; Li, X. X.; Lin, L. D.; Wang, G.; Zhang, Z.; Li, L.; Yu, Y. Layered rare earth-organic framework as highly efficient luminescent matrix: the crystal structure, optical spectroscopy, electronic transition, and luminescent sensing properties. *Cryst. Growth Des.* **2019**, 19, 4754–4764.
- (20) Zhang, Z.; Fang, Q. H.; Zhuang, Z. Y.; Han, Y.; Li, L. Y.; Yu, Y. Europium activated aluminum organic frameworks for highly selective and sensitive detection of Fe³⁺ and Cr(VI) in aqueous solution. *Chin. J. Struct. Chem.* **2020**, 39, 1958–1964.
- (21) Zhao, H. X.; Liu, L. Q.; Liu, Z. D.; Wang, Y.; Zhao, X. J.; Huang, C. Z. Highly selective detection of phosphate in very complicated matrixes with an off-on fluorescent probe of europium-adjusted carbon dots. *Chem. Commun.* **2011**, 47, 2604–2606.
- (22) Binnemans, K. Interpretation of europium(III) spectra. *Coord. Chem. Rev.* **2015**, 295, 1–45.
- (23) Wen, G. X.; Wu, Y. P.; Dong, W. W.; Zhao, J.; Li, D. S.; Zhang, J. An ultrastable europium(III) organic framework with the capacity of discriminating Fe²⁺/Fe³⁺ ions in various solutions. *Inorg. Chem.* **2016**, 55, 10114–10117.
- (24) Zheng, X.; Ren, S.; Wang, L.; Gai, Q.; Dong, Q.; Liu, W. Controllable functionalization of carbon dots as fluorescent sensors for independent Cr(VI), Fe(III) and Cu(II) ions detection. *J. Photochem. Photobiol., A* **2021**, 417, 113359–113365.
- (25) Barrio Manso, J. L.; Calvo, P.; García, F. C.; Pablos, J. L.; Torroba, T.; García, J. M. Functional fluorescent aramids: aromatic polyamides containing a dipicolinic acid derivative as luminescent converters and sensory materials for the fluorescence detection and quantification of Cr(VI), Fe(III) and Cu(II). *Polym. Chem.* **2013**, 4, 4256–4264.
- (26) Guo, X. Y.; Dong, Z. P.; Zhao, F.; Liu, Z. L.; Wang, Y. Q. Zinc(II)-organic framework as a multi-responsive photoluminescence sensor for efficient and recyclable detection of pesticide 2,6-dichloro-4-nitroaniline, Fe(III) and Cr(VI). *New J. Chem.* **2019**, 43, 2353–2361.
- (27) Chen, Y.; Liu, G.; Wang, X.; Lu, X.; Xu, N.; Chang, Z.; Zhang, Z.; Li, X. Various carboxylates induced eight Zn(II)/Cd(II) coordination polymers with fluorescence sensing activities for Fe(III), Cr(VI) and oxytetracycline. *CrystEngComm* **2021**, 23, 8077–8086.
- (28) Chen, Z.; Mi, X.; Wang, S.; Lu, J.; Li, Y.; Li, D.; Dou, J. Two novel penetrating coordination polymers based on flexible S-containing dicarboxylate acid with sensing properties towards Fe³⁺ and Cr₂O₇²⁻ ions. *J. Solid State Chem.* **2018**, 261, 75–85.
- (29) Chen, Z.; Mi, X.; Lu, J.; Wang, S.; Li, Y.; Dou, J.; Li, D. From 2D → 3D interpenetration to packing: N coligand-driven structural assembly and tuning of luminescent sensing activities towards Fe³⁺ and Cr₂O₇²⁻ ions. *Dalton Trans.* **2018**, 47, 6240–6249.
- (30) Zhou, A. M.; Wei, H.; Gao, W.; Liu, J. P.; Zhang, X. M. Two 2D multi-responsive luminescence coordination polymers for selective sensing of Fe³⁺, Cr^{VI} anions and TNP in aqueous medium. *CrystEngComm* **2019**, 21, 5185–5194.
- (31) Lin, Y.; Zhang, X.; Chen, W.; Shi, W.; Cheng, P. Three cadmium coordination polymers with carboxylate and pyridine mixed ligands: luminescent sensors for Fe^{III} and Cr^{VI} ions in an aqueous medium. *Inorg. Chem.* **2017**, 56, 11768–11778.
- (32) Singh, M.; Senthilkumar, S.; Rajput, S.; Neogi, S. Pore-functionalized and hydrolytically robust Cd(II)-metal-organic framework for highly selective, multicyclic CO₂ adsorption and fast-responsive luminescent monitoring of Fe(III) and Cr(VI) ions with notable sensitivity and reusability. *Inorg. Chem.* **2020**, 59, 3012–3025.
- (33) Cui, L.; Li, Y.; Gan, Y.; Feng, Q.; Long, J. Syntheses, structure and luminescent sensing for Cr(VI)/Fe(III) of a Zn(II) coordination polymer. *J. Mol. Struct.* **2020**, 1200, 126797–126802.
- (34) Dao, X.; Ni, Y.; Pan, H. MIL-53(Al)/Eu³⁺ luminescent nanocrystals: solvent-adjusted shape-controllable synthesis and highly selective detections for Fe³⁺ ions, Cr₂O₇²⁻ anions and acetone. *Sens. Actuators, B* **2018**, 271, 33–43.
- (35) Jia, P.; Wang, Z.; Zhang, Y.; Zhang, D.; Gao, W.; Su, Y.; Li, Y.; Yang, C. Selective sensing of Fe³⁺ ions in aqueous solution by a biodegradable platform based lanthanide metal organic framework. *Spectrochim. Acta, Part A* **2020**, 230, 118084–118091.
- (36) Xu, N.; Zhang, Q.; Hou, B.; Cheng, Q.; Zhang, G. A novel magnesium metal-organic framework as a multiresponsive luminescent sensor for Fe(III) ions, pesticides, and antibiotics with high selectivity and sensitivity. *Inorg. Chem.* **2018**, 57, 13330–13340.
- (37) Dang, S.; Ma, E.; Sun, Z. M.; Zhang, H. A layer-structured Eu-MOF as a highly selective fluorescent probe for Fe³⁺ detection through a cation-exchange approach. *J. Mater. Chem.* **2012**, 22, 16920–16926.
- (38) Zheng, M.; Tan, H.; Xie, Z.; Zhang, L.; Jing, X.; Sun, Z. Fast response and high sensitivity europium metal organic framework fluorescent probe with chelating terpyridine sites for Fe³⁺. *ACS Appl. Mater. Interfaces* **2013**, 5, 1078–1083.
- (39) Zhou, Y.; Chen, H. H.; Yan, B. An Eu³⁺ post-functionalized nanosized metal-organic framework for cation exchange-based Fe³⁺-sensing in an aqueous environment. *J. Mater. Chem. A* **2014**, 2, 13691–13697.

Received: December 31, 2021

Accepted: February 18, 2022

Published: April 8, 2022